

## Dissolved inorganic phosphorus export to the coastal zone: Results from a spatially explicit, global model

John A. Harrison,<sup>1</sup> Sybil P. Seitzinger,<sup>1</sup> A. F. Bouwman,<sup>2</sup> Nina F. Caraco,<sup>3</sup>  
Arthur H. W. Beusen,<sup>2</sup> and Charles J. Vörösmarty<sup>4</sup>

Received 18 August 2004; revised 9 November 2004; accepted 2 February 2005; published 27 August 2005.

[1] Here we describe, test, and apply a spatially explicit, global model of river-borne dissolved inorganic phosphorus (DIP) export called NEWS-DIP. Among the innovations in NEWS-DIP are increased spatial resolution ( $0.5 \times 0.5^\circ$ ), explicit treatment of sewage, fertilizer, manure, and weathering P sources, and inclusion of reservoir retention and consumptive water use terms. The NEWS-DIP model performed better than pre-existing global models in predicting DIP yield for both calibration and validation basins ( $r^2 = 0.72$  and  $0.56$ , respectively). NEWS-DIP predicts that of the  $34 \text{ Tg of P yr}^{-1}$  loaded on watersheds by human activity globally, approximately 3% reaches river mouths as DIP; anthropogenic sources account for 65% ( $0.71 \text{ Tg yr}^{-1}$ ) of the DIP exported to the coastal zone, with the remainder ( $0.38 \text{ Tg yr}^{-1}$ ) attributable to natural weathering processes; DIP yields range over 5 orders of magnitude, from less than  $0.01$  to  $1153 \text{ kg P km}^{-2} \text{ yr}^{-1}$  with highest predicted DIP yields clustering in East Asia, Europe, and Indonesia; human sewage is the largest anthropogenic source of DIP to the coastal zone on all continents and to all ocean basins. NEWS-DIP also suggests that despite regional variability, at the global scale, non-point sources of DIP such as inorganic P fertilizer and manure are much less important in determining coastal export of DIP than point sources and natural weathering processes.

**Citation:** Harrison, J. A., S. P. Seitzinger, A. F. Bouwman, N. F. Caraco, A. H. W. Beusen, and C. J. Vörösmarty (2005), Dissolved inorganic phosphorus export to the coastal zone: Results from a spatially explicit, global model, *Global Biogeochem. Cycles*, 19, GB4S03, doi:10.1029/2004GB002357.

### 1. Introduction

[2] The global phosphorus (P) cycle has been greatly altered by human activity. P mining and subsequent use as fertilizer has more than doubled P inputs to the environment over natural, background P from weathering [Mackenzie *et al.*, 1998; Bennett *et al.*, 2001; Fixen and West, 2002]. Commonly a limiting nutrient in lakes and other freshwater systems, P is also thought to play an important role in controlling coastal primary productivity and ecosystem dynamics. Though coastal systems are typically thought of as nitrogen (N)-limited, there are several coastal systems where P-limitation has been demonstrated for all or part of the year [Harrison *et al.*, 1990; Jensen *et al.*, 1998; Fisher *et al.*, 1999; Murrell *et al.*, 2002], and coastal P-limitation may well become more prevalent if anthropogenic N

mobilization increases faster than P mobilization, with projected increases in food and energy production [Justic *et al.*, 1995; Turner *et al.*, 2003].

[3] In many systems, dissolved inorganic P (DIP) (also called soluble reactive phosphorus (SRP) or orthophosphate ( $\text{PO}_4^{3-}$ )) constitutes a relatively small portion of the phosphorus exported by rivers ( $\sim 1.5 \text{ Tg P}$  as DIP globally versus  $\sim 20 \text{ Tg P}$  as total P (TP) globally [Meybeck, 1982; Melack, 1995]). However, whereas all of the DIP pool is generally thought to be bioavailable in rivers, lakes, and coastal waters, significant portions of the particulate and organic P pools are not available for use by organisms [Bradford and Peters, 1987; Ekholm, 1994; Fox, 1989]. Therefore, even accounting for desorption of sorbed P in estuaries [Froelich, 1988; Howarth *et al.*, 1995], DIP plays an important role in controlling the biology of such systems. As such, the development of a DIP export model constitutes a critical first step toward a synthetic understanding of coastal P delivery, which must eventually also include models for delivery of particulate and dissolved organic P.

[4] Several studies have modeled the dynamics of river DIP transport at local to regional scales with mixed success (Table 1). The more successful DIP models [e.g., Weller *et al.*, 2003] have been developed for specific regions and have been highly tuned to conditions within those regions. It is therefore not feasible to apply these models at the

<sup>1</sup>Institute of Marine and Coastal Sciences, Rutgers–The State University, New Brunswick, New Jersey, USA.

<sup>2</sup>Netherlands Environmental Assessment Agency (MNP), Bilthoven, Netherlands.

<sup>3</sup>Institute of Ecosystem Studies, Millbrook, New York, USA.

<sup>4</sup>Water Systems Analysis Group, Complex Systems Research Center, Institute for the Study of Earth, Oceans, and Space, University of New Hampshire, Durham, New Hampshire, USA.

**Table 1.** Description and Performance Evaluation of Existing DIP-Export Models<sup>a</sup>

Model Name and/or Reference	Model Scale <sup>b</sup>	Number of Sites to Which Calibrated/in Which Validated	Region(s) of Application <sup>c</sup>	$r^2$			Model Type <sup>d</sup>
				Concentration, mg L <sup>-1</sup>	Yield, kg km <sup>-2</sup> yr <sup>-1</sup>	Load, kg basin <sup>-1</sup> yr <sup>-1</sup>	
Patuxent model [Weller et al., 2003]	catchment	21 catchments in one basin/0	Patuxent R. (U.S.)	0.73	0.84	0.994	empirical
Riverstrahler [Billen et al., 2001]	river reach	3 stations on one river/0	Seine R. (Europe)	0.39	NA	NA	dynamic
LASCAM [Viney et al., 2000]	catchment	2 catchments in one basin/0	Avon R. (Australia)	NA	NA	NA	dynamic
McIntyre et al. [2003]	river reach	1/0	Charles R. (U.S.)	0.68	NA	NA	dynamic
Daly et al. [2002]	catchment	35 catchments on 12 rivers/0	Ireland	0.68 and 0.62 <sup>e</sup>	NA	NA	empirical
Arheimer and Liden [2000]	catchment	24 catchments in one region/4 catchments	Sweden	0.71	NA	NA	empirical
Caraco [1995]	river basin	32 large rivers worldwide/0	Global	NA	0.67	NA	quasi-empirical
Smith et al. [2003]	river basin	165 large and small rivers worldwide/0	Global	NA	0.58	NA	empirical
NEWS-DIP (this paper)	river basin	53 medium-large rivers worldwide/54 medium-large rivers worldwide	Global	0.42	0.72	0.74	quasi-empirical

<sup>a</sup>Coefficients of determination ( $r^2$  values) are for log-modeled versus log-measured DIP concentrations (both annual average and instantaneous depending on the model), and are calculated for calibration data sets. Some commonly used water quality models which reportedly model DIP export such as HSPF [Bicknell et al., 1997], QUAL2E [Chapra and Pelletier, 2003], SWAT [Neitsch et al., 2002], and WASP [Wool et al., 2004] have not been included in this table because of a lack of published comparisons between modeled and measured DIP data. NA denotes not available in literature.

<sup>b</sup>Model scale is defined by the finest spatial unit for which the model predicts DIP export.

<sup>c</sup>Region(s) of application refers to the system(s) in which each model has been applied to predict DIP export.

<sup>d</sup>Model type refers to whether the model is purely empirical, quasi-empirical, or dynamic. Empirical models were derived entirely from a multiple regression approach. Quasi-empirical models were developed using literature and data-derived relationships and tuned to natural systems via adjustable coefficients. Dynamic models are similar to quasi-empirical models in that they have been developed using observed relationships and tuned to particular systems. However, these models can be run through time.

<sup>e</sup>Data set was divided into two groups based on principal components analysis, and distinct groups were modeled separately.

global scale. Until relatively recently, a similar situation existed with respect to dissolved inorganic N (DIN). However, the recent development and application of global, spatially explicit DIN and total N export models [Seitzinger and Kroeze, 1998; Kroeze and Seitzinger, 1998; Caraco and Cole, 1999; Seitzinger et al., 2002; Green et al., 2004] has facilitated the development of the first global, spatially explicit representations of DIN export by rivers to the coastal zone.

[5] To this point, there has not been a comparable analysis of the magnitude, distribution, and sources of DIP export via rivers. While the global, and in some cases regional, magnitude of TP and DIP export has been estimated using measurement data [e.g., Pierrou, 1975; Meybeck, 1982; Richey, 1983; Wollast, 1983; Howarth et al., 1996; Smith et al., 2003], and Ver et al. [1999] include DIP in their non-spatially explicit global model of nutrient export, global spatial patterns of DIP export remain largely unstudied. Caraco [1995] developed a model for DIP export by large rivers using urban population density, fertilizer P inputs, and basin runoff as explanatory variables, but did not apply that model to non-calibration basins. Smith et al. [2003] developed an empirical model of DIP yield, predicting DIP yield as a function of water runoff and population density. However, this model was not validated using non-calibration rivers,

and was only used to define broad classes of basins with respect to DIP yield. It also cannot be used to examine the relative importance of different DIP sources within a watershed.

[6] Here we describe, test, and apply a new, spatially explicit global model of DIP export. This model was developed as part of an international interdisciplinary effort to model river export of multiple bioactive elements (C, N, P, and Si) and elemental forms (dissolved/particulate, inorganic/organic) called Global Nutrient Export from Watersheds (Global NEWS). Because of this, we hereinafter refer to the DIP model as “NEWS-DIP.” NEWS-DIP includes several innovations and advantages over previous global DIP export models, including increased spatial resolution ( $0.5 \times 0.5^\circ$ ) of global input data sets and watershed delineations, explicit treatment of sewage, fertilizer, manure, and weathering P sources, and inclusion of reservoir retention and consumptive water use terms.

## 2. Methodology

[7] We developed and applied the NEWS-DIP model to estimate the global distribution, magnitudes, and sources of DIP export by rivers worldwide for the year 1995. In the sections that follow, we describe the NEWS-DIP

**Table 2.** Input Data Sets for NEWS-DIP

Data Set	Resolution	Year	Source(s)
Basin delineations	0.5°	1960–1994	STN30 [Vörösmarty et al., 2000a, 2000b]
River networks	0.5°	1960–1994	STN30 [Vörösmarty et al., 2000a, 2000b]
Water runoff	0.5°	1960–1994	STN30 [Vörösmarty et al., 2000a, 2000b]
Population density	0.5°	1995	Klein Goldewijk [2001]
Fertilizer P inputs	0.5°	1995	Bouwman et al. [2005a]
Manure P inputs	0.5°	1995	Bouwman et al. [2005a]
Land use	0.5°	1995	Bouwman et al. [2005a]
Country GNP	country	1995	World Bank [2000]
Sanitation data sets	country	1995	WHO/UNICEF [2001]; Bouwman et al. [2005b]
Sewage treatment	country	1995	WHO/UNICEF [2001]; Bouwman et al. [2005b]
Pre-dam water discharge	137 rivers	NA	Meybeck and Ragu [1996]

model, the model calibration procedure used in model development, and model input data, calibration data, and validation data.

## 2.1. NEWS-DIP Model

[8] Building on work by Caraco [1995], we developed a new model to predict DIP yield ( $\text{kg P km}^{-2} \text{ yr}^{-1}$ ). This model predicts DIP yield ( $DIP$ ) as a function of point source and non-point source P inputs, weathered P, reservoir retention, and consumptive use. The model's central equation is as follows:

$$DIP = (Q_{act}/Q_{nat}) \times (1 - D) \times \left\{ H \times E_{cap} + \left[ 1 / \left( 1 + (R/a)^{-b} \right) \right] \times \left[ W_{max} + L_{max} \times (P_{fert} + P_{am}) \right] \right\}, \quad (1)$$

where  $DIP$  is the area-weighted mean DIP yield ( $\text{kg P km}^{-2} \text{ yr}^{-1}$ ) for an entire river basin (as opposed to DIP-load ( $\text{kg P basin}^{-1} \text{ yr}^{-1}$ ) or DIP concentration ( $\text{mg P-L}^{-1}$ )).  $DIP$  is calculated as a function of within-basin P sources and sinks. Source terms include point sources and diffuse sources. Point sources are calculated as a function of population density ( $H$ ) (individuals  $\text{km}^{-2}$ ) and per-capita DIP yield ( $E_{cap}$ ) ( $\text{kg P person}^{-1} \text{ yr}^{-1}$ ). Diffuse sources are calculated as a function of runoff ( $R$ ) ( $\text{m yr}^{-1}$ ), fertilizer P inputs ( $P_{fert}$ ) ( $\text{kg P km}^{-2} \text{ yr}^{-1}$ ), animal manure P inputs ( $P_{am}$ ) ( $\text{kg P km}^{-2} \text{ yr}^{-1}$ ), and four calibrated coefficients defining the shape of the runoff response curve for weathering and non-point DIP sources ( $a$ ,  $b$ ,  $W_{max}$ , and  $L_{max}$ , discussed further in section 2.2.2). Diffuse sources were treated as a sigmoid function of runoff, increasing slowly with runoff at low runoff values, more rapidly with runoff at higher runoffs, and topping out at a threshold level in high runoff systems. This sigmoid relationship between runoff and diffuse sources is responsible for the term  $(1/(1 + (R/a)^{-b}))$  in NEWS-DIP's central equation. Sinks include consumptive water use, calculated as the ratio of contemporary river discharge ( $Q_{act}$ ) to pre-dam river discharge ( $Q_{nat}$ ), and within-basin DIP retention due to DIP trapping in reservoirs ( $D$ ) (0–1). Input variables consisted mainly of spatially explicit,  $0.5^\circ \times 0.5^\circ$  resolution gridded data sets (Table 2), which were used to compute area-weighted, basin wide means. Several of the model inputs were derived from submodels described in the following sections. Calibrated coefficients  $a$ ,  $b$ ,  $W_{max}$ , and  $L_{max}$ , were constrained to observation-based ranges (section 2.2.2), and in our formulation were set to 0.85, 2, 26, and 0.04, respectively.

[9] The magnitudes of individual source contributions were calculated as follows:

$$DIP_{\text{point source}} = (Q_{act}/Q_{nat}) \times (1 - D) \times H \times E_{cap}, \quad (2)$$

$$DIP_{\text{weathering}} = (Q_{act}/Q_{nat}) \times (1 - D) \times \left\{ W_{max} / \left[ 1 + (R/a)^{-b} \right] \right\}, \quad (3)$$

$$DIP_{\text{fertilizer}} = (Q_{act}/Q_{nat}) \times (1 - D) \times \left\{ L_{max} \times P_{fert} / \left[ 1 + (R/a)^{-b} \right] \right\}, \quad (4)$$

$$DIP_{\text{manure}} = (Q_{act}/Q_{nat}) \times (1 - D) \times \left\{ L_{max} \times P_{man} / \left[ 1 + (R/a)^{-b} \right] \right\}, \quad (5)$$

where symbols and coefficient values are the same as in equation (1) and the notation section.

## 2.2. Model Development

### 2.2.1. River Data

[10] River discharge and DIP concentration data were compiled for 111 medium-to-large sized river basins worldwide from several sources (Appendix A). Rivers used for model calibration and validation included basins from a broad range of latitudes, climate types, and sizes (Figure 1; Appendix A). They also included river basins that were both heavily developed and relatively free of human activity. Runoff in study basins ranged from 0.01 to 2.75  $\text{m yr}^{-1}$  with a median value of 0.28  $\text{m yr}^{-1}$ . Median annual DIP concentration ([DIP]) ranged from 0.002 to 0.810  $\text{mg L}^{-1}$  with a median value of 0.030 for all systems. When possible, we used flow-weighted mean [DIP] in our analysis (17 cases). When this was not possible, we used median [DIP] (90 cases) or mean concentrations (four cases). The combined discharge of study rivers accounts for over 50% of the world river exoreic discharge (37,400  $\text{km}^3 \text{ yr}^{-1}$  [Meybeck, 1982]), with 37% in the calibration data set, and 14% in the validation data set.

[11] We applied several filters to the available data to assure quality and appropriate application. We included only data where we could verify that both flows and concentrations had been measured (i.e., were not model-derived). We limited our analysis to concentration and

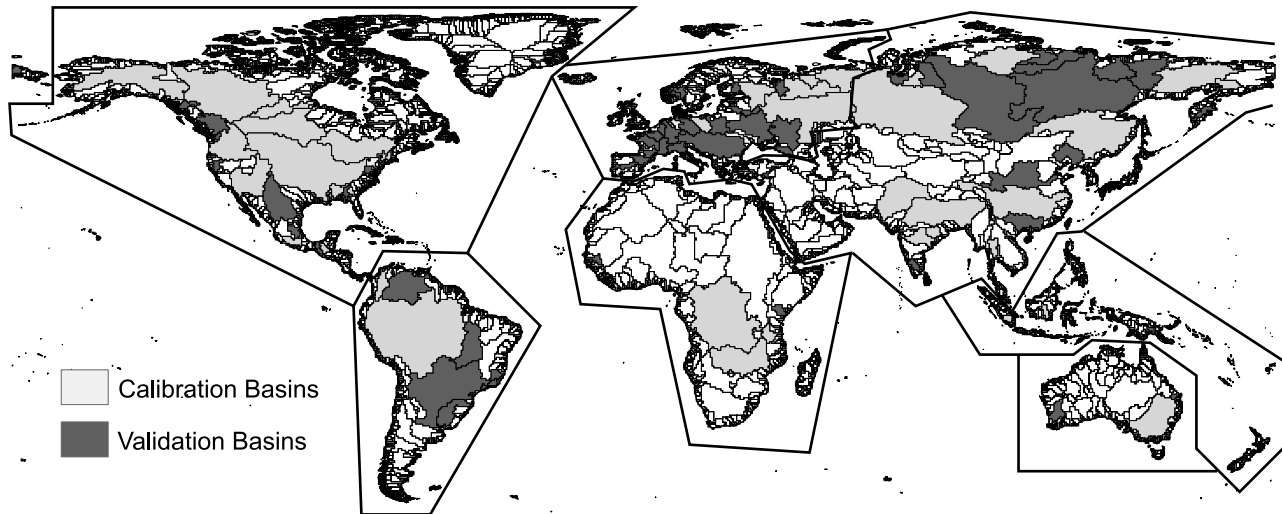


**Figure 1.** Spatial distribution of basins used to calibrate and validate the NEWS-DIP model. Bold lines represent approximate borders used to delineate continents for continental scale aggregations. See Appendix A for data, model output, and basin names.

discharge data that had been collected after 1970. We also limited our calibration and validation analyses to basins that encompassed more than ten  $0.5 \times 0.5$  degree grid cells (see section 2.2.3.). We selected the most seaward, freshwater sampling point on each river included in our study, and the great majority of stations were located within 50 km of the coast. We also limited our analysis to exorheic river basins, basins exporting water to one of the major oceans, the Mediterranean Sea, or the Black Sea. Rivers discharging to the Baltic Sea were treated as discharging to the Atlantic Ocean.

[12] In addition to the 111 medium-large basins used for model calibration and validation, we also used data from 393 smaller basins in the continental United States (each containing fewer than ten  $0.5 \times 0.5^\circ$  grid cells; range 70–38616 km<sup>2</sup>) to test NEWS-DIP’s ability to predict DIP load for smaller watersheds. These data were taken from the same sources and subject to the same quality control filters as the medium and large-sized basins.

### 2.2.2. Model Calibration, Validation, and Sensitivity Analysis

[13] For the NEWS-DIP model, approximately half of the basins (56 rivers) in our global river data set were randomly assigned as calibration rivers (Figure 1). Calibration was achieved by optimizing the model to attain the highest model efficiency ( $R^2$ ) while maintaining coefficients within the range of literature values. Model efficiency (capital  $R^2$ , not the coefficient of determination ( $r^2$ )) is a metric ranging from 0 to 1 reflecting the degree of fit between measured and modeled values [Nash and Sutcliffe, 1970]. When  $R^2 = 1$ , all points fall on the 1:1 line. When  $R^2$  is 0, model error is equal to the variability in the data. Coefficients  $a$ ,  $b$ ,  $L_{\max}$ , and  $W_{\max}$  were the only calibrated coefficients in the NEWS-DIP model. No coefficients relating to point source inputs or reservoir retention were calibrated.

[14] We determined the potential ranges for coefficients  $a$ ,  $b$ ,  $W_{\max}$ , and  $L_{\max}$  through analysis of published data.

Coefficients  $a$  and  $b$  determine the inflection point and the steepness of the curve relating non-point source P (including weathered P) to water runoff.  $W_{\max}$  defines the upper limit for weathering derived DIP (kg P km<sup>-2</sup> yr<sup>-1</sup>).  $L_{\max}$  defines the upper limit for the fraction of applied manure and P fertilizer that is carried downstream. To determine the ranges of  $a$ ,  $b$ , and  $W_{\max}$  (as well as the shape of the relationship between runoff and weathering-derived P), we examined published data for P export from basins receiving low levels (<100 kg km<sup>-2</sup> yr<sup>-1</sup>) of anthropogenic P. For these basins, there appeared to be a sigmoid relationship between runoff and DIP yield, with an inflection point somewhere between 0 and 1 m yr<sup>-1</sup> runoff. We therefore allowed the inflection point of modeled DIP yield (defined by  $a$ ) to vary between 0 and 1, with a step size of 0.05. We allowed  $b$  (defining the steepness of the rising arm of the sigmoid curve in the relationship between runoff and weathered P export) to vary between 1 and 20, with a step size of 1. In these relatively uninhabited basins, P-yield never exceeded 40 kg P km<sup>-2</sup> yr<sup>-1</sup>. Therefore, in our model calibration procedure, we allowed  $W_{\max}$  to vary between 10 and 40 kg km<sup>-2</sup> yr<sup>-1</sup> with a step size of 2.

[15] We assumed that non-point P would respond similarly to weathered P (i.e., as the same function of runoff), and therefore applied the same  $a$  and  $b$  to our representation of non-point P mobilization as was applied to our representation of weathering-derived P. The maximum non-point P mobilized ( $L_{\max}$ ) is treated as a fraction of the non-point P (fertilizer and manure) applied. We determined the potential range of  $L_{\max}$  based on literature values. Plot-level and regional studies have generally found that about 0.1–3.3% of the P applied as fertilizer or manure is lost as DIP via surface water transport [Burwell et al., 1997; McColl et al., 1977; Nicholaichuk and Read, 1978; Sharpley and Syers, 1979; McDowell and McGregor, 1984; Sharpley et al., 1995; Bennett et al., 1999; Baker and Richards, 2002]. However, these studies have generally not been

conducted in areas subject to high runoff rates, and the fraction of applied P fertilizer and manure lost to surface waters as DIP is likely to be higher in such systems. Also, with respect to manure, this percentage can vary substantially depending on livestock diet, soil sorption capacity, and runoff. Reported values for export of DIP from manure treated under ideal conditions for DIP loss (P-rich manure, no conservation tillage, and intense, artificial rain events) range up to 40% [Ebeling *et al.*, 2002]. For this study, we allowed  $L_{\max}$  to vary between 1 and 10% with a step size of 1%. We then used a script to test every possible combination of these coefficients, and chose the set of coefficient values yielding the highest  $R^2$ .

[16] The 55 basins that had not been used for model calibration were assigned to a validation data set. We used this data set to evaluate NEWS-DIP bias and precision according to Alexander *et al.* [2002]. Prediction error ( $K$ ) is expressed, as by Alexander *et al.* [2002], as

$$K = \left[ \frac{L - M}{M} \times 100 \right], \quad (6)$$

where  $L$  is the model prediction, and  $M$  is the measured stream DIP export.

[17] Change in model efficiency ( $R^2$ ) [Nash and Sutcliffe, 1970] was determined upon removal of model components (e.g., point sources, non-point sources, weathering sources, consumptive use, and reservoir DIP retention). This change in model efficiency was then used to evaluate the relative importance of different model components in explaining DIP export. We also subjected the NEWS-DIP model to a sensitivity analysis in which we varied each model input and coefficient and each combination of inputs and coefficients ( $\pm 5\%$ ) and quantified model response to these variations.

[18] In addition to our work with NEWS-DIP, we also evaluated  $r^2$ ,  $R^2$ , model bias, and model precision of two other DIP export models. One of these was a model recently published by Smith *et al.* [2003], developed as a product of the International Geosphere Biosphere Program-Land Ocean Interactions in the Coastal Zone (IGBP-LOICZ) project and hereinafter referred to as LOICZ-DIP. LOICZ-DIP model predictions were compared with measurement data not used in the formulation of the original LOICZ-DIP model. We carried out a similar analysis for a quasi-empirical model developed for large rivers [Caraco, 1995] (hereinafter referred to as CARACO-DIP); this model used literature values to constrain coefficients for a model that is consistent with physical drivers of DIP export, but was not validated using non-calibration data. In analysis of both models, we used 47 river basins with more than 10 cells each, all coinciding with basins used to validate NEWS-DIP. However, eight basins in the data set used to validate NEWS-DIP were excluded from LOICZ-DIP and CARACO-DIP validation data sets because they were used in the original calibration of those models. We used SPSS 11.5.1 for basic statistical procedures and Matlab 6.0 for model calibration and  $R^2$  calculations.

### 2.2.3. Hydrological Inputs and Reservoir Retention

[19] An updated version of the STN30-p global river network (STN30-p version 6.0 [Vörösmarty *et al.*, 2000a,

2000b]) was used to define basin boundaries for model runs at  $0.5 \times 0.5^\circ$  resolution. Because we were limited to  $0.5 \times 0.5^\circ$  resolution, and because basins were delineated using a digital elevation model, STN30-p basin shape and size deviated somewhat from actual basin shape and size. This problem worsened as basins decreased in size. For example, for basins encompassing more than ten  $0.5^\circ \times 0.5^\circ$  grid cells, the average ratio of modeled to measured basin size was  $1.18 \pm 0.48$  (1 S.D.). However, for basins with fewer than ten  $0.5^\circ \times 0.5^\circ$  grid cells, the average ratio of modeled to measured basin size was generally too high and quite variable ( $7.14 \pm 28.98$  (1 S.D.)) We therefore limited our calibration and validation analyses to basins that contained more than 10  $0.5 \times 0.5^\circ$  degree grid cells. We used modeled runoff estimates from the water balance model (WBM) as described by Vörösmarty *et al.* [2000a, 2000b] to supply runoff values for model runs.

[20] To estimate the impact of consumptive water (and thus DIP) use on DIP export, we multiplied predicted DIP yield by the ratio of measured post-dam water discharge to measured pre-dam water discharge ( $Q_{act}/Q_{nat}$ ). Values for  $Q_{act}/Q_{nat}$  were taken from Meybeck and Ragu [1996], and when unavailable were assumed to equal 1. This approach assumes that DIP removed from rivers for irrigation or other consumptive purpose does not find its way back into surface drainage waters.

[21] For our estimate of DIP retention by reservoirs, we used a spatially explicit dam database [Vörösmarty *et al.*, 1997]. This database includes locations and reservoir volumes for 714 large ( $>15$  m tall) dams worldwide. We calculated P retention in reservoirs ( $D$ ) according to Wilhelmus *et al.* [1978] as

$$D = 0.85 \times \left( 1 - e^{(-0.0807 \times Rt)} \right), \quad (7)$$

where  $Rt$  is the change in retention time (days) due to the creation of reservoirs, calculated by dividing reservoir capacity by reservoir discharge as done by Vörösmarty *et al.* [2003]. However, rather than clustering reservoirs by sub-basin as done by Vörösmarty *et al.* [2003], we evaluated  $Rt$  for every reservoir for which we had data. This approach may somewhat overestimate the impact of reservoirs when reservoirs occur in sequence and relatively close together. It may also underestimate the impact of reservoirs by failing to include smaller, but potentially important, impoundments. However, this approach represents a marked improvement over ignoring reservoirs altogether as previous models have done.

### 2.2.4. Point Source Inputs

[22] Point sources are critically important in defining DIP export by many rivers. Previous global DIP models have included point sources as major drivers of DIP export, but have relied solely on population density [Smith *et al.*, 2003] or estimated urban population density [Caraco, 1995] as predictors of DIP point sources, ignoring potentially important factors such as variability in P excretion rates, sewerage, and wastewater treatment. P excretion rates, sewerage, and wastewater treatment all vary substantially at the global scale [World Health Organization (WHO)/UNICEF, 2001; Bouwman *et al.*, 2005b], so including them in an

estimate of point source inputs is likely to enhance model predictive capacity. We calculated net DIP point source emission to surface water similarly to *Bouwman et al.* [2005a] as

$$E_{cap} = (1 - T) \times I \times (0.365 \times P_{em}), \quad (8)$$

where  $E_{cap}$  is net phosphorus emission to surface water ( $\text{kg person}^{-1} \text{ yr}^{-1}$ ),  $T$  is the rate of P removal via wastewater treatment (i.e., P retention as a fraction of the P influent to treatment plants; 0–1),  $I$  is the fraction of the population connected to sewerage systems (0–1), and  $P_{em}$  is the gross human P emission ( $\text{g P person}^{-1} \text{ d}^{-1}$ ). In addition to sewage, P-based detergents may constitute a significant source of surface water DIP in many countries. However, they are not explicitly accounted for by NEWS-DIP owing to a lack of input data.

[23] We used a conceptual relationship of per capita human P emission and per capita income similar to that used by *Van Drecht et al.* [2003] for nitrogen,

$$P_{em} = 3.2 + 4.4 \times (\text{GDP}/43,639)^{0.5}, \quad (9)$$

where  $P_{em}$  is per capita daily human P emission ( $\text{g person per day}$ ) and GDP is per capita gross domestic product (1995 US\$ per capita per year). GDP for each country is divided by 43,639, the world's highest per capita GDP in 1995 (Switzerland) [*World Bank*, 2000]. Low-income countries have human per capita P emissions of about  $1.3 \text{ kg yr}^{-1}$  and industrialized countries between  $2.3$  and  $2.6 \text{ kg yr}^{-1}$ . Data for  $I$  (equation (8)) were extracted from *Bouwman et al.* [2005b].

[24] For countries where sewage treatment data were available (16% of countries globally),  $T$  was calculated as

$$T = 0.1 \times F_{mech} + 0.35 \times F_{biol} + 0.8 \times F_{adv}, \quad (10)$$

where  $F_{mech}$ ,  $F_{biol}$ , and  $F_{adv}$  are the fractions of each country's sewage that has mechanical, biological, and advanced treatment, respectively. Coefficients for each treatment type (0.1, 0.35, and 0.8) were assigned as suggested by *Black and Veach Consulting Engineers* [1971] and *Slam* [1980]. For countries where no data on sewage treatment were available we used regional estimates of sewage treatment [*WHO/UNICEF*, 2001; *Bouwman et al.*, 2005b].

### 2.2.5. Diffuse P Sources

[25] There is some indication that non-point P inputs such as fertilizer and manure are important sources of DIP to surface waters during runoff events [*Ebeling et al.*, 2002; *Baker and Richards*, 2002] at local to regional scales. However, manure and fertilizer P inputs have not explicitly been included in past efforts to model DIP export at the global scale. In NEWS-DIP, P inputs from inorganic P fertilizer ( $P_{fe}$ ) and animal manure ( $P_{am}$ ) were calculated as done by *Bouwman et al.* [2005a]. For fertilizer P inputs, national P-use data were used and distributed across agricultural areas, maintaining different application rates for different crop types as done by *Bouwman et al.* [2005a].

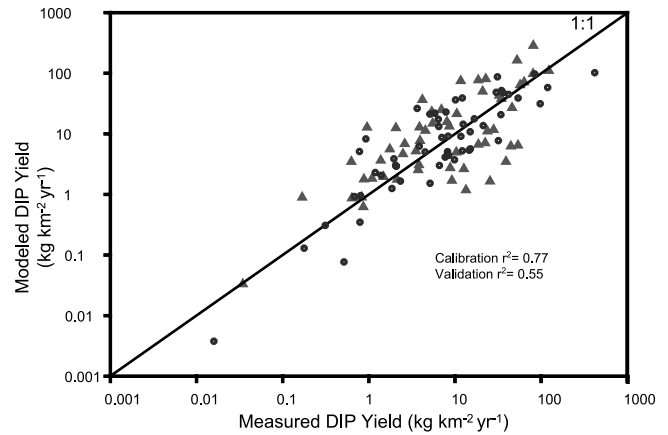


**Figure 2.** Measured versus modeled DIP yield ( $\text{kg km}^{-2} \text{ yr}^{-1}$ ) for calibration basins (circles) and validation basins (triangles). See Appendix A for data, model output, and basin names. The 1:1 line is shown.

For manure P inputs, we used published N:P ratios of manure for various livestock species, including pigs, cows, chickens, sheep, goats, and horses [*Bouwman et al.*, 2005a].

## 3. Results and Discussion

### 3.1. NEWS-DIP Model Performance

[26] NEWS-DIP explains 72% and 56% of the variability in per-area DIP export (DIP-yield) in calibration and validation basins, respectively, substantially more than previous global models of DIP export (Figure 2, Tables 1 and 3). It explains 74% and 61% of the variability in per-basin DIP export (DIP load) in calibration and validation basins, respectively (Table 3). Slopes of measured versus modeled DIP yield were not significantly different from unity for calibration or validation basins ( $P > 0.05$ ). Using modeled (i.e., STN30) rather than measured runoff values for basins with measured DIP had very little effect on the predictive capacity of the model ( $r^2$  using modeled runoff for measured versus predicted DIP yield = 0.72 and 0.54 for the calibration and validation data sets, respectively).

[27] Despite the reasonably good fit between measured and modeled DIP yield (or load), error on a basin-by-basin scale was considerable. The standard error of log-transformed predictions was 0.47. DIP yield predictions for 59% of basins were within a factor of 2 of measurement-based estimates, 73% were within a factor of 4, and 96% were within 1 order of magnitude. Error in DIP yield predictions associated with large basins was similar to error associated with relatively small basins. However, absolute error associated with high-yield basins was somewhat greater than error associated with low-yield basins as evidenced by the similar scatter in data points relative to the 1:1 line over the entire range despite log-log axes (Figure 2). The range of errors in NEWS-DIP predictions is substantially smaller than that for other

**Table 3.** Metrics of Model Performance for NEWS-DIP, LOICZ, and CARACO Models Validated With Data From a Global Data Set<sup>a</sup>

Model	DIP or DIN Yield, kg P or Nkm <sup>-2</sup> yr <sup>-1</sup>		DIP Load, Ton P basin <sup>-1</sup>		IQR <sup>b</sup>	Prediction Errors, %			
	<i>r</i> <sup>2</sup>	<i>R</i> <sup>2</sup>	<i>r</i> <sup>2</sup>	<i>R</i> <sup>2</sup>		Minimum	25th	75th	Maximum
NEWS-DIP-Calibration	0.72	0.68	0.74	0.63	178	-86	-31	148	1494
NEWS-DIP-Validation	0.56	0.51	0.60	0.47	247	-90	-9	239	2542
LOICZ-DIP-Validation	0.46	0.17	0.52	0.46	502	-78	-16	487	13672
CARACO-Validation	0.41	0.34	0.54	0.43	692	-96	30	722	19982
N-Model-Calibration <sup>c</sup>	0.84				108	-77	-26	82	1205

<sup>a</sup>*R*<sup>2</sup> is model efficiency as defined in section 2.2.2, and *r*<sup>2</sup> is the coefficient of determination. Measured runoff from basins containing more than ten  $0.5 \times 0.5^\circ$  cells were used for all validation calculations. N-Model error statistics for calibration basins are also included for comparison of global DIP models with a global DIN model. Errors are computed as the difference between the predicted and measured values of stream phosphorus yield ( $\text{kg km}^{-2} \text{yr}^{-1}$ ) expressed as a percentage of the measured export (equation (6)).

<sup>b</sup>Interquartile range (difference between the 25th and 75th percentiles of the distribution of errors).

<sup>c</sup>Values for *Seitzinger and Kroeze* [1998] N-model for DIN, from *Alexander et al.* [2002].

DIP export models, as indicated by the inter-quartile range and distribution of prediction errors (Table 3).

[28] NEWS-DIP's uncertainty, as reflected in its inter-quartile range and distribution of prediction errors, is slightly greater than uncertainty associated with global export models for TN and DIN (Table 3) [*Alexander et al.*, 2002]. However, the error associated with NEWS-DIP is similar in magnitude to the interannual variability of DIP yields in several U.S. rivers. For example, the difference between minimum and maximum DIP export years is fivefold for the Mississippi River and over an order of magnitude for the Potomac River (data from *Alexander et al.* [1996]). This suggests that NEWS-DIP predictions are likely to fall within the range of interannual variability for any given river.

[29] Despite the uncertainty inherent in global modeling efforts, the NEWS-DIP model represents a substantial improvement over past efforts at DIP export modeling. In the sections that follow, we use the NEWS-DIP model

to gain insight into patterns, controls, and sources of DIP export from watersheds worldwide. We then explore model sensitivities, uncertainties, and potential ways to improve our capacity to model DIP export in future modeling efforts.

### 3.2. Model Predictions

#### 3.2.1. Spatial Distribution of DIP Export and Sources

[30] Predicted DIP yields ranged over 5 orders of magnitude, from less than  $0.01$  to  $1153 \text{ kg P km}^{-2} \text{yr}^{-1}$  (Figures 2 and 3). Highest predicted DIP yields tended to cluster in Japan, Korea, Indonesia, and Europe. There are also predicted hot spots for DIP yield in portions of the northeast United States, Central and South America, and West Africa. The highest predicted yield occurs in Japan's Kiso basin. The lowest predicted yield occurs in Northern Australia. In general, low predicted DIP yields tend to occur in areas with low levels of anthropogenic influence or in relatively dry regions.

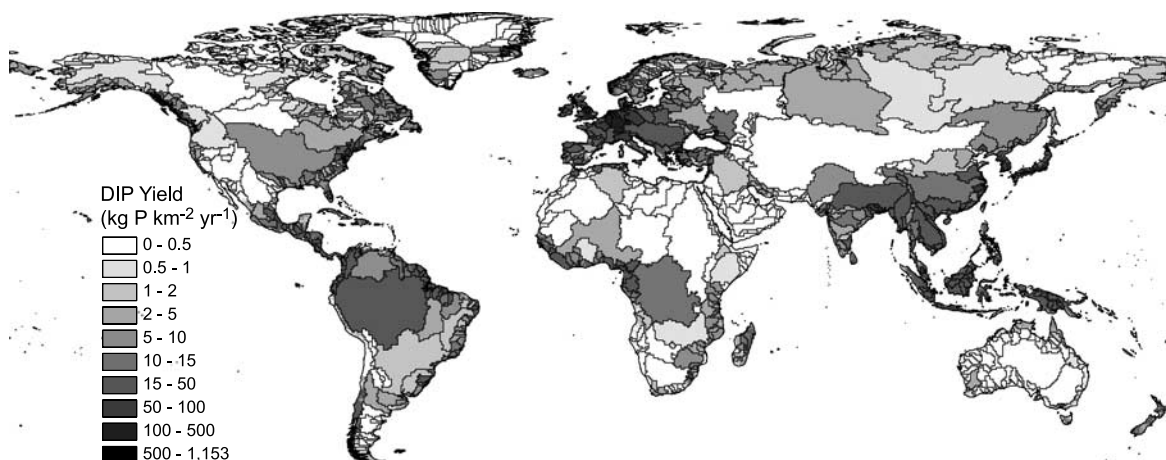


**Figure 3.** NEWS-DIP predicted DIP yield by watershed ( $\text{kg P km}^{-2} \text{yr}^{-1}$ ) for exoreic basins. White basins are either endoreic or had no predicted DIP export. For the sake of clarity, only delineations for basins containing more than 10 half-degree grid cells are shown. See color version of this figure at back of this issue.

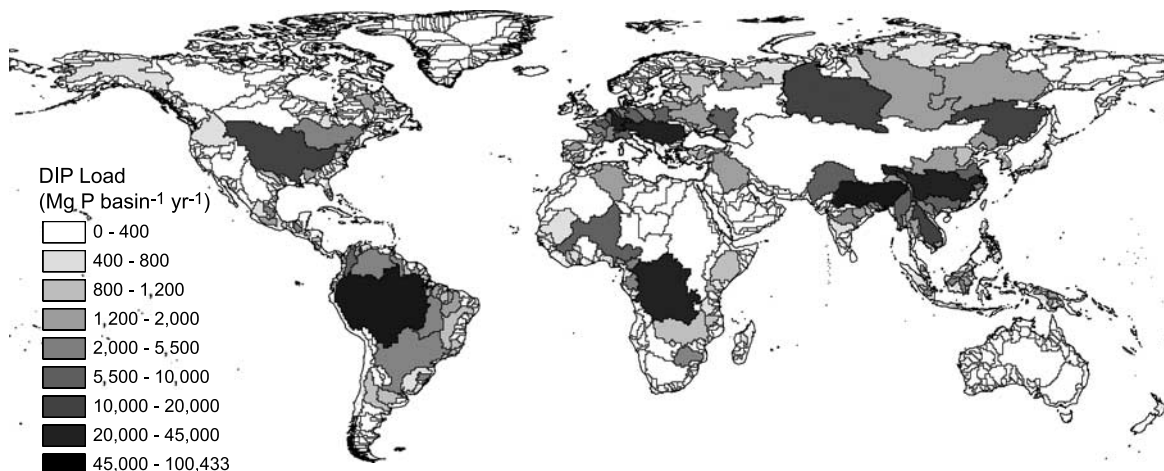


**Figure 4.** NEWS-DIP predicted DIP load by watershed ( $\text{Mg P basin}^{-1} \text{ yr}^{-1}$ ) for exoreic basins. For the sake of clarity, only delineations for basins containing more than 10 half-degree grid cells are shown. See color version of this figure at back of this issue.

[31] The pattern of predicted coastal DIP loads differs in a number of respects from the pattern of predicted DIP yield (compare Figures 3 and 4). This is consistent with the observation made by *Smith et al.* [2003] that while locally important because of their effects on receiving waters, high yield systems do not dominate DIP export on a global scale. Whereas the five highest yield systems account for just 0.03% of the total DIP export to the coastal zone, the five highest load systems (the Amazon ( $100,432 \text{ Mg P yr}^{-1}$ ), Ganges ( $45,415 \text{ Mg P yr}^{-1}$ ), Zaire ( $37,622 \text{ Mg P yr}^{-1}$ ), Danube ( $24,018 \text{ Mg P yr}^{-1}$ ), and Chang Jiang ( $20,482 \text{ Mg P yr}^{-1}$ ) rivers) together account for over 20% of the predicted global DIP export. The largest 10% of river basins as defined by STN30 account for 62% of the globally exported DIP.

[32] NEWS-DIP predicts that in 1995, weathering was the dominant source of coastal DIP in 71% of STN30's exoreic basins (Figure 5). Basins where NEWS-DIP predicts weathering to dominate DIP sources lie in high-latitude regions with relatively little human influence and in wet tropical systems such as the Amazon, the Congo, Northern Australia, and Indonesia. NEWS-DIP predicts that human activity dominated DIP export from basins encompassing 29% of exoreic basins worldwide, and that DIP export in 99% of these basins is dominated by human sewage. These point-source dominated basins include the majority of the temperate, tropical, and subtropical river basins (Figure 5). NEWS-DIP also predicts that inorganic P fertilizer is the dominant source of DIP to the coast in just 1.2% of STN30 basins. These basins are small and located in New Zealand, Japan, and Southeast Asia (Figure 6). Manure was not predicted to be the dominant source of coastal DIP in any watersheds as defined by STN30.

[33] Though a few studies have attempted to attribute sources of TP [*Boynton et al.*, 1995; *Baker and Richards*,

2002; *Moore et al.*, 2004] and total  $\text{PO}_4$  (dissolved plus acid-soluble, but undigested particulate) [*Jordan et al.*, 2003] to river P loading, we were able to locate only one study quantifying the relative importance of different land-based sources specifically to river DIP loading. This one study of a relatively rural portion of the Thames River watershed [*Cooper et al.*, 2002] suggests that point sources account for 77–97% of the river DIP inputs, depending on the year (1995–1999). NEWS-DIP predicts that for the whole Thames River watershed, including the more urban portions, point sources account for 99% of the DIP loading, a fairly good agreement with the local study.

[34] Comparison of NEWS-DIP predictions with regional studies that estimate sources of other P forms also suggests that NEWS-DIP predictions are reasonable. Studies attributing TP or total  $\text{PO}_4$  to point and non-point sources have calculated point source inputs based on data from wastewater treatment plants and subtracted that value from total export to calculate contribution from non-point sources. Such studies have estimated that point sources contribute 95% of the TP load to the Patuxent River [*Boynton et al.*, 1995] and 50% of the TP load to Baltic rivers [*HELCOM*, 2003]. Assuming TP:DIP ratios of 0.033 and 1 for point and non-point sources, respectively (similar to values reported by *Cooper et al.* [2002] for the Thames), this translates to estimated point source contributions of 97 and 67% for the Patuxent and Baltic, respectively. NEWS-DIP estimates that point sources account for 99 and 92% of the DIP source in the Patuxent and Baltic regions, respectively.

[35] Our work with NEWS-DIP suggests that on a global scale, point sources, not anthropogenic diffuse sources, most often dominate DIP export to coastal regions, even in intensively farmed regions. This suggests that sources of river-exported DIP differ substantially from sources of river-exported DIN. Whereas global DIN export has been

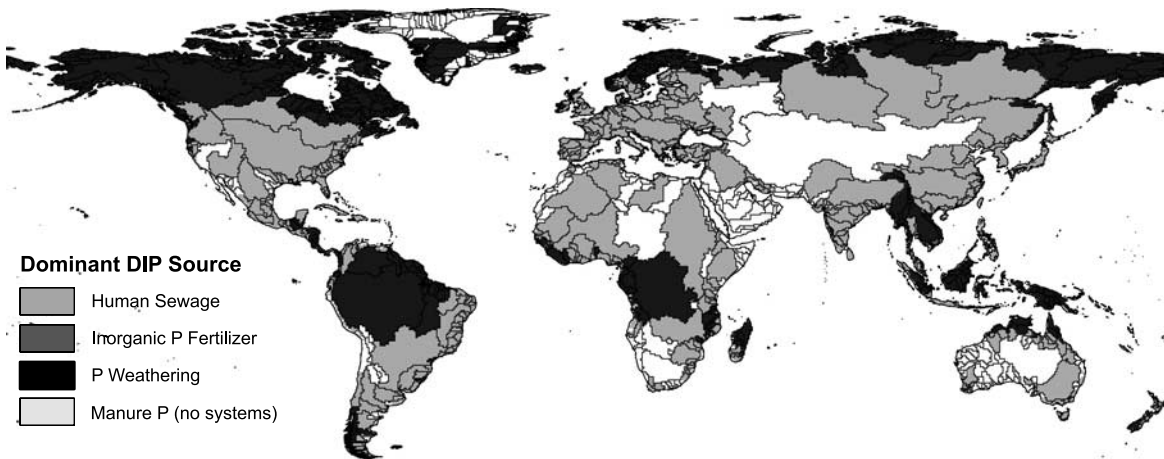


**Figure 5.** Dominant source of DIP by watershed for exoreic basins. “Dominant source” is defined as the modeled source that NEWS-DIP predicts contributes the largest fraction of DIP to the coast. For the sake of clarity, only delineations for basins containing more than 10 half-degree grid cells are shown. See color version of this figure at back of this issue.

attributed mainly to non-point N sources, particularly N fertilizer [Seitzinger and Kroeze, 1998; Caraco and Cole, 1999; Green et al., 2004; Dumont et al., 2005], global DIP export is influenced mainly by sewage point sources. The dominant role of point sources in controlling DIP export is consistent with previous global analyses [Caraco, 1995; Smith et al., 2003].

**3.2.2. Global and Regional Analyses**

[36] We estimate that 1.1 Tg P yr<sup>-1</sup> reached river mouths as DIP in 1995. This estimate is similar to other recent, measurement-based and model-calculated estimates of global DIP export, which range from 0.8 to 2.4 Tg yr<sup>-1</sup> [Pierrou, 1975; Meybeck, 1982; Richey, 1983; Wollast, 1983; Smith et al., 2003]. Of the 35 Tg of P we calculate are loaded on watersheds by human activity globally, we estimate approximately 3% is exported by rivers as DIP. According to NEWS-DIP, anthropogenic sources account for 65% (0.7 Tg yr<sup>-1</sup>) of the DIP exported to the coastal zone, with the remainder (0.4 Tg yr<sup>-1</sup>) attributable to natural weathering processes. This predicted rate of weathering-derived P export is similar to the rate predicted by Meybeck [1982] (0.4 Tg yr<sup>-1</sup>), an estimate based on a study of relatively unimpacted rivers.

[37] According to NEWS-DIP, sewage waste alone accounts for over half (61%) of the total global DIP export via rivers. Inorganic fertilizer (4%) and animal manure (0.5%) contribute substantially smaller fractions of the coastal DIP load.

[38] According to NEWS-DIP predictions, Asia is the largest continental exporter of DIP (Figure 6), contributing 32% (0.35 Tg yr<sup>-1</sup>) of the total global DIP export to the coast. Export rates for other continents vary substantially, with Europe, South America, North America (including Greenland), Africa, Oceania (including New Zealand), and Australia each exporting 0.20, 0.20, 0.12, 0.12, 0.09, and 0.01 Tg of DIP P yr<sup>-1</sup>, respectively. Of the world’s ocean

basins, NEWS-DIP predicts that the Atlantic Ocean receives the most DIP from land-based sources (0.48 Tg yr<sup>-1</sup>), followed by the Pacific and Indian oceans (0.32 and 0.16, respectively), the Mediterranean and Black seas (0.10 Tg yr<sup>-1</sup>), and the Arctic Ocean (0.03 Tg yr<sup>-1</sup>).

[39] Continental and ocean basin calculations suggest that humans have outstripped natural processes as a source of DIP to the coast on the majority of continents and ocean basins (Figure 6). However, natural DIP sources still out-

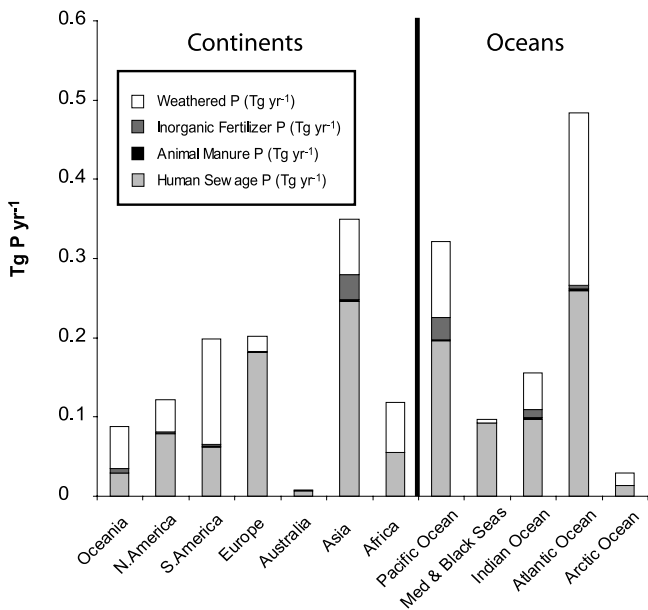


**Figure 6.** River export of DIP (Tg P yr<sup>-1</sup>) from continents and to ocean basins. Relative influence of various P sources are calculated according to NEWS-DIP.

strip anthropogenic DIP sources to the Arctic Ocean, and are approximately equal in the Atlantic Ocean. Weathering is still the principal source of DIP in South America, Africa, and Oceania. However, rapid economic development and population growth within these regions mean that anthropogenic DIP sources may well outstrip weathering as a source of DIP to coastal waters within the next several decades in these areas as well. According to NEWS-DIP, on every continent and in every ocean basin, human sewage is by far the largest source of anthropogenically derived exported DIP. However, fertilizer inputs are relatively more important in Asia and Oceania than on other continents (Figure 6).

### 3.3. Sources of Uncertainty, Assumptions, and Future Directions

[40] The NEWS-DIP model represents a significant step forward in terms of capacity to model river DIP export at the global scale. However, there is still much room for model improvement. As global data sets improve, there will be opportunities to greatly improve estimates of river DIP export. In the following two sections, we use patterns of model error along with model efficiency and sensitivity analyses (Tables 4 and 5) to infer where improvements to global data sets and model improvements are likely to be most useful in enhancing DIP yield estimates. We also examine the potential implications of assumptions made during the model development process, and suggest future directions in the field of global nutrient modeling.

#### 3.3.1. Model Efficiency and Sensitivity

[41] An analysis of model efficiency, wherein model components were removed sequentially to evaluate the contribution of each to model predictive capacity, suggests that weathering and sewage point source sub-models are particularly important model drivers. This analysis suggests that consumptive water use also plays a role in the correct determination of DIP yield by NEWS-DIP, but that non-point source and reservoir retention terms, while important in certain cases, are less vital in explaining DIP yield than other model components at the global scale (Table 4).

[42] A sensitivity analysis of NEWS-DIP in which model inputs and coefficients were varied by  $\pm 5\%$  in order to

**Table 4.** Model Efficiencies for Comparison of Log-Transformed Measured and Model-Predicted DIP Yield, Using NEWS-DIP With Various Components Removed<sup>a</sup>

Treatment	Model Efficiency ( $R^2$ )	Percent Change in Model Efficiency Resulting From Component Removal
Complete model	0.51	0
No sewage point sources	-0.16	-136
No weathering	-2.25	-539
No consumptive use	0.45	-11
No reservoir retention	0.53	+3
No non-point sources	0.50	-0.7

<sup>a</sup>Only results using validation basins are included here, but similar patterns hold for analyses of calibration data and of all available data.

**Table 5.** Results of a Sensitivity Analysis Indicating Mean and Maximum Change in Predicted DIP Yield as a Function of Increasing Input Data Sets and Model Parameters by +5%

Parameter or Input	Mean Change in Predicted DIP, $\text{kg km}^{-2} \text{yr}^{-1}$ , %
Percent retention in reservoirs	6.27
$W_{\max}$	4.49
Runoff, m	3.00
Population density, indiv./ $\text{km}^2$	2.97
Per Capita P, $\text{kg}/\text{indiv.}/\text{yr}$	2.97
$a$	1.88
Fertilizer P	0.12
$L_{\max}$	0.15
$b$	0.10
Manure P	0.03

evaluate model response (Table 5) suggested that the NEWS-DIP model is fairly robust. With the exception of the parameter  $D$  (% retention in reservoirs; equation (1)), 5% changes in all input parameters, coefficients, and all possible combinations of coefficients result in average changes in predicted DIP yield of less than 5%, and in most cases substantially less. NEWS-DIP predictions are particularly sensitive to small changes to  $D$  in highly engineered systems such as the Rio Grande and Colorado rivers.

[43] NEWS-DIP predictions are also fairly sensitive to small changes in the weathering-related parameters  $W_{\max}$ ,  $R$ ,  $a$  and  $b$  (Table 5). The weathering sub-model also plays an important role in model efficiency (Table 4). The NEWS-DIP weathering submodel (equation (3)) does a reasonably good job in predicting DIP export from relatively human-free systems (anthropogenic P inputs  $< 100 \text{ kg km}^{-2} \text{ yr}^{-1}$ ) ( $r^2$  of log-transformed measured and modeled DIP yield = 0.63,  $r^2$  of load = 0.81). However, NEWS-DIP's sensitivity to changes in the weathering submodel coefficients suggests that any improvement in NEWS-DIP's representation of weathering-derived P is likely to improve model fit.

[44] Model efficiency analysis also suggests that consumptive water use is an important component of the NEWS-DIP model (Table 4). NEWS-DIP currently assumes that there is no consumptive use in systems without consumptive use data. This means that NEWS-DIP is likely to overestimate DIP export from systems where there is significant water consumption, but no consumptive use data. This overestimate is likely to be most pronounced in developing arid regions with irrigated agriculture.

[45] Finally, NEWS-DIP output is relatively insensitive to removal of its non-point P source term (Table 4) and to manipulation of non-point source input data sets (Table 5). This suggests that inaccuracies in fertilizer and manure input data sets have relatively minor impacts on model predictions, especially in comparison with inaccuracies associated with other model inputs.

#### 3.3.2. Future Directions

[46] Taken together, model efficiency and sensitivity analyses suggest several areas for future improvements in NEWS-DIP. For example, model efficiency and sensitivity analyses both suggest that point-sources are important in

driving predictions of DIP export (Table 4). Though the NEWS-DIP approach represents a significant enhancement over past estimate techniques, there is still much room for improvement in estimates of global P-excretion, sewage connectivity, and sewage treatment. Including data on P-based detergent use may also improve estimates of point source P inputs.

[47] Model efficiency and sensitivity analyses also suggest that NEWS-DIP predictions are sensitive to estimates of weathering (Tables 4 and 5). In future DIP export models, it may be possible to reduce uncertainty in estimates of weathering rates by refining the NEWS-DIP sub-model for predicting weathering-derived P (equation (3)) through the inclusion of factors thought to influence weathering rates such as temperature, soil type, soil parent material, and pH as improved global data sets become available.

[48] NEWS-DIP predictions are also quite sensitive to small changes in the retention term  $D$  (equation (1); Table 5), particularly in highly engineered systems, and DIP retention is one of the most poorly constrained model inputs. In future global DIP export models it will be important to improve representation of reservoir retention. Including DIP sinks other than reservoirs and consumptive water use may also improve the accuracy of future models. For example, natural lakes and river-associated wetlands may account for significant levels of DIP retention, but are not treated explicitly by the NEWS-DIP model. Retention on land may also constitute an important DIP sink as re-use of sewage as fertilizer (night soil), conservation tillage practices, and highly weathered, P-deficient soils, and P-limited terrestrial (or aquatic) ecosystems all may lead to DIP retention within watersheds. However, terrestrial DIP retention was not included explicitly in this version of the NEWS-DIP model owing to a lack of sufficient input data.

[49] Though our analysis is currently limited to basins containing more than ten  $0.5 \times 0.5^\circ$  grid cells, this problem will most likely be solved incrementally as increasingly reliable, finer resolution spatial data sets of model-drivers become available. In the United States, where finer-scale data on land-use and watershed delineations are available, NEWS-DIP maintains predictive ability substantially below the threshold created by the resolution of STN30 and other  $0.5^\circ$  global data sets. For example, NEWS-DIP explained 56% of the variability in DIP yield and 62% of the variability in DIP load from 327 small ( $<20,000 \text{ km}^2$ ; approximately equal to 10 half-degree grid cells at midlatitudes) USGS-monitored basins when finer resolution input data were used [Alexander *et al.*, 1996]. However, NEWS-DIP only explained 23% of the variability in DIP yield and 34% of the variability in DIP load from small ( $<20,000 \text{ km}^2$ ) basins when  $0.5 \times 0.5^\circ$  global input data sets were used. This suggests that some of the uncertainty associated with NEWS-DIP predictions is due to the limited resolution of input data sets. With improved resolution and quality of input and validation data sets and the development of hydrological models that route water and materials downstream through river networks, it will become possible to improve the spatial resolution of DIP export models. This improved input and validation data will likely improve model fit significantly. Higher resolution validation data

and the development of sub-basin-scale models will facilitate the enhanced representation of DIP retention as well as the inclusion of interactions between elements and elemental forms. Also, as improved temporal resolution data sets of runoff and land-use become available, it will be possible to use NEWS-DIP to examine sub-annual patterns of DIP export. Incorporating such sub-basin spatial and sub-annual temporal variability into global DIP export modeling efforts will constitute significant advances in understanding of the global P cycle and effects. However, for now, NEWS-DIP represents a significant advancement in its own right as the first spatially explicit, global DIP export model with the capacity to attribute DIP to natural and anthropogenic sources.

## Appendix A

[50] Table A1 includes data used in NEWS-DIP calibration and validation as well as NEWS-DIP predictions. Columns include river names, continents, watershed area ( $\text{km}^2$ ), annual runoff (m), DIP concentrations ( $\text{mg P L}^{-1}$ ), sources of concentration and discharge data, basin population density, rates of per capita P excretion ( $\text{kg P individual}^{-1} \text{ yr}^{-1}$ ), manure P production ( $\text{kg P ha}^{-1} \text{ yr}^{-1}$ ), and inorganic fertilizer P application ( $\text{kg P ha}^{-1} \text{ yr}^{-1}$ ), and model-predicted DIP yield ( $\text{kg P km}^{-2} \text{ yr}^{-1}$ ).

## Notation

[51] The following is a list of variables and their definitions for NEWS-DIP model.

$DIP$	DIP yield, $\text{kg P km}^{-2} \text{ yr}^{-1}$ .
$DIP_{\text{point source}}$	DIP yield from point sources, $\text{kg P km}^{-2} \text{ yr}^{-1}$ .
$DIP_{\text{weathering}}$	DIP yield from natural weathering sources, $\text{kg P km}^{-2} \text{ yr}^{-1}$ .
$DIP_{\text{fertilizer}}$	DIP yield from inorganic P fertilizer, $\text{kg P km}^{-2} \text{ yr}^{-1}$ .
$DIP_{\text{manure}}$	DIP yield from livestock manure, $\text{kg P km}^{-2} \text{ yr}^{-1}$ .
$Q_{\text{act}}$	Measured discharge after dam construction, $\text{km}^3 \text{ H}_2\text{O yr}^{-1}$ .
$Q_{\text{nat}}$	Measured discharge prior to dam construction, $\text{km}^3 \text{ H}_2\text{O yr}^{-1}$ .
$D$	Fraction DIP retained in reservoirs (0–1).
$H$	Human population density, individuals $\text{km}^{-2}$ .
$E_{\text{cap}}$	Per capita DIP yield, $\text{kg P individual}^{-1} \text{ yr}^{-1}$ .
$R$	Runoff, $\text{m H}_2\text{O yr}^{-1}$ .
$a$	Unit-less coefficient defining how non-point DIP and weathered DIP respond to runoff; for NEWS-DIP set equal to 0.6.
$b$	Unit-less coefficient defining how non-point DIP and weathered DIP respond to runoff; for NEWS-DIP set equal to 2.
$W_{\text{max}}$	Maximum DIP yield due to weathering alone ( $\text{kg P km}^{-2} \text{ yr}^{-1}$ ); for NEWS-DIP set equal to 12.

**Table A1.** Data for NEWS-DIP Calibration and Validation Rivers

River	Continent	Basin Area, km <sup>2</sup>	Runoff, m yr <sup>-1</sup>	DIP, mg P L <sup>-1</sup>	Source <sup>a</sup>	Population, indiv. km <sup>-2</sup>	Per Capita P, kg P indiv. <sup>-1</sup> yr <sup>-1</sup>	Manure P, kg P ha <sup>-1</sup> yr <sup>-1</sup>	Inorg. Fert. P, kg P ha <sup>-1</sup> yr <sup>-1</sup>	NEWS-DIP, kg P km <sup>-2</sup> yr <sup>-1</sup>
Alabama	North America	114789	0.604	0.010	3	14.91	0.35	2.45	1.02	21.22
Altamaha	North America	36260	0.353	0.026	5	34.24	0.37	3.44	2.18	15.69
Amazon	South America	6112000	1.078	0.022	6	4.31	0.29	0.56	0.04	17.29
Amguema	Asia	29600	0.311	0.012	1	0.00	0.28	0.00	0.00	3.08
Amur	Asia	1855000	0.185	0.021	1	34.88	0.23	2.15	2.05	8.92
Anabar	Asia	79000	0.172	0.002	2	0.00	0.46	0.00	0.00	1.00
Apalachicola Bay	North America	51451	0.568	0.006	3	56.99	0.34	1.76	1.14	5.74
Balsas	North America	112000	0.125	0.095	1	165.19	0.35	4.89	0.06	10.65
Barito	Asia	66000	1.315	0.005	1	24.07	0.13	0.00	0.00	24.64
Bug	Europe	63700	0.053	0.097	1	64.54	0.32	2.85	0.01	22.99
Cauweri	Asia	88000	0.238	0.100	1	347.36	0.05	7.99	2.38	8.61
Chao Phrya	Asia	111435	0.249	0.026	1	97.70	0.14	4.23	2.77	10.94
Chiang Jiang	Asia	1808000	0.513	0.020	7	219.72	0.07	9.01	6.25	16.34
Churchill (Hud.)	North America	298000	0.134	0.006	1	0.14	0.33	0.28	0.22	0.07
Colorado (Ari.)	North America	639000	0.029	0.100	5	11.47	0.40	0.25	0.30	0.00
Columbia	North America	669000	0.353	0.014	5	7.84	0.35	1.30	1.07	1.12
Connecticut	North America	25019	0.679	0.030	5	95.37	0.40	0.05	0.15	28.81
Dalalven	Europe	25000	0.608	0.002	1	11.31	0.19	0.00	0.00	6.63
Danube	Europe	805000	0.252	0.183	8	103.08	0.18	5.52	1.83	30.21
Daugava	Europe	87900	0.229	0.037	1	34.32	0.29	2.24	0.00	12.07
Dnepr	Europe	504000	0.106	0.036	1	63.74	0.31	3.10	0.06	2.96
Dnestr	Europe	72100	0.148	0.056	1	100.18	0.28	2.88	0.00	4.90
Don	Europe	422000	0.067	0.042	1	47.41	0.36	3.89	0.00	13.60
Drammenselva	Europe	17000	0.606	0.002	1	28.05	0.36	0.00	0.00	13.68
Eastmain	North America	46400	0.619	0.022	1	0.00	0.29	0.00	0.00	1.72
Ebro	Europe	84000	0.217	0.115	4	39.62	0.42	7.00	3.12	2.34
Elbe	Europe	146000	0.162	0.390	1	162.18	0.39	10.87	2.59	63.94
Evros	Europe	55000	0.124	0.280	4	68.88	0.30	3.05	1.30	19.49
Fraser	North America	220000	0.518	0.050	1	7.78	0.35	0.71	0.41	1.36
Fuchun Jiang	Asia	54349	0.686	0.046	1	433.46	0.08	6.63	5.54	56.37
Gambia	Africa	42000	0.117	0.015	1	19.19	0.29	2.29	-0.02	5.14
Ganges	Asia	1050000	0.470	0.075	1	266.50	0.09	7.48	1.52	25.13
Garonne	Europe	55000	0.313	0.104	1	57.56	0.47	6.89	2.04	31.24
Glama	Europe	41200	0.558	0.008	1	31.08	0.34	0.00	0.00	16.06
Grijalva	North America	36400	0.632	0.085	1	62.30	0.41	3.13	0.33	5.04
Guadiana	Europe	72000	0.125	0.057	1	26.53	0.37	5.52	3.45	10.84
Hunter	Australia	21411	0.022	0.062	3	5.74	0.63	0.70	0.27	0.89
Huang He	Asia	752000	0.055	0.020	1	138.05	0.08	2.89	2.81	1.68
Hudson	North America	34700	0.565	0.060	8	154.37	0.40	0.69	0.21	39.10
Indigirka	Asia	305000	0.176	0.010	2	0.02	0.41	0.00	0.00	1.01
Indus	Asia	916000	0.098	0.520	1	142.33	0.11	3.66	1.78	6.06
Kamchatka	Asia	55900	0.592	0.075	1	0.93	0.34	0.00	0.00	8.77
Khatanga	Asia	364000	0.277	0.006	1	0.81	0.38	0.00	0.00	2.12
Klamath	North America	31339	0.517	0.027	5	5.29	0.33	0.24	0.85	9.90
Kolyma	Asia	526000	0.243	0.010	2	0.01	0.47	0.00	0.00	1.11
Kuban	Europe	57900	0.235	0.030	1	56.06	0.41	2.11	0.00	25.88
Kymjoki	Europe	37200	0.257	0.010	1	18.09	0.11	1.71	1.08	3.85
Lena	Asia	2430000	0.219	0.007	2	0.97	0.38	0.02	0.00	1.93
Liao	Asia	219000	0.074	0.053	1	122.86	0.09	4.01	4.22	6.35
Loire	Europe	112000	0.254	0.090	1	69.48	0.47	13.47	6.15	30.95
Luan	Asia	54000	0.078	0.012	1	119.93	0.06	2.49	2.50	9.85
MacKensie	North America	1787000	0.175	0.004	1	0.16	0.31	0.06	0.03	0.99
Magdalena	South America	235000	1.009	0.120	1	73.44	0.36	6.70	0.64	40.41
Mahanadi	Asia	52094	0.972	0.038	3	174.69	0.16	11.06	2.39	14.35
Meuse	Europe	29000	0.352	0.230	1	281.99	0.81	25.40	3.46	158.77
Mezen	Europe	56000	0.495	0.027	2	2.25	0.49	0.00	0.00	5.35
Mississippi	North America	2916081	0.199	0.085	5	19.99	0.35	5.70	3.36	6.64
Murray	Australia	1060000	0.022	0.024	1	0.95	0.43	2.45	0.50	0.28
Musi	Asia	56700	1.418	0.030	1	68.73	0.12	3.21	1.13	42.51
N. Dvina	Europe	348000	0.302	0.039	1	4.30	0.38	0.55	0.08	5.65
Nadym	Asia	48000	0.400	0.154	2	2.00	0.44	0.00	0.00	3.64
Nelson	North America	1132000	0.074	0.004	1	4.30	0.32	2.31	1.61	0.28
Nemanus	Europe	98200	0.200	0.046	1	39.46	0.29	7.08	0.54	9.42
Neva	Europe	282000	0.278	0.030	1	27.38	0.33	0.36	0.00	4.19
Ob	Europe	2950000	0.137	0.072	2	8.40	0.34	1.24	0.03	3.79
Odra	Europe	112000	0.163	0.370	1	118.81	0.31	8.04	3.50	32.61
Olenek	Asia	198000	0.174	0.008	2	0.05	0.42	0.00	0.00	0.96
Onega	Europe	12000	1.317	0.009	2	2.90	1.78	0.91	0.21	19.78

Table A1. (continued)

River	Continent	Basin Area, km <sup>2</sup>	Runoff, m yr <sup>-1</sup>	DIP, mg P L <sup>-1</sup>	Source <sup>a</sup>	Population, indiv. km <sup>-2</sup>	Per Capita P, kg P indiv. <sup>-1</sup> yr <sup>-1</sup>	Manure P, kg P ha <sup>-1</sup> yr <sup>-1</sup>	Inorg. Fert. P, kg P ha <sup>-1</sup> yr <sup>-1</sup>	NEWS-DIP, kg P km <sup>-2</sup> yr <sup>-1</sup>
Orinocco	South America	1100000	1.032	0.010	1	9.98	0.36	1.74	0.11	4.14
Panuco	North America	66300	0.261	0.016	1	70.32	0.44	2.87	0.18	35.01
Paraiba Do Sul	South America	57000	0.537	0.010	1	78.38	0.36	5.82	0.82	14.07
Parana	South America	2783000	0.204	0.045	1	21.08	0.33	4.02	0.34	1.62
Pechora	Europe	312000	0.413	0.035	2	3.22	0.37	0.01	0.00	5.94
Peel	North America	71000	0.345	0.006	1	0.00	0.35	0.00	0.00	3.68
Penzhina	Asia	71600	0.317	0.021	1	0.78	0.44	0.00	0.00	3.23
Po	Europe	70000	0.657	0.075	1	211.07	0.44	7.46	7.07	77.18
Potomac	North America	29966	0.367	0.031	5	82.71	0.41	3.78	1.56	56.17
Purari	Asia	30580	2.751	0.002	1	8.18	0.08	0.41	0.00	25.14
Rhine	Europe	224000	0.310	0.400	1	284.47	0.29	15.59	2.98	119.32
Rhone	Europe	95600	0.627	0.101	4	97.39	0.45	5.29	2.41	44.61
Rio Grande (U.S.)	North America	456702	0.039	0.021	5	13.19	0.56	0.97	0.17	0.02
Rufiji	Africa	178000	0.198	0.010	1	21.63	0.10	0.45	0.00	3.56
Sacramento	North America	70000	0.293	0.030	1	14.94	0.27	2.03	1.09	2.29
Saint Lawrence	North America	1025000	0.330	0.046	8	55.63	0.33	1.49	1.09	3.89
Sakarya	Asia	55300	0.106	0.160	1	76.85	0.34	5.00	3.54	19.67
Scheldt	Europe	11400	0.526	0.810	1	383.34	0.95	27.71	4.83	39.20
Seine	Europe	78600	0.201	0.400	1	205.07	0.42	9.28	4.62	97.86
Severnaya Dvina	Europe	348000	0.303	0.023	2	4.30	0.38	0.55	0.08	5.42
Seyhan	Asia	19300	0.249	0.010	1	65.01	0.42	1.31	1.30	4.21
Skagit	Europe	8011	1.872	0.012	5	56.89	0.82	3.65	1.30	22.32
Stikine	North America	51593	0.979	0.018	5	0.00	0.32	0.00	0.00	19.88
Susquehanna	North America	71000	0.532	0.010	5	61.65	0.31	1.32	0.68	22.98
Swan Canning	Australia	126021	0.010	0.060	3	5.97	0.58	0.58	0.29	2.20
Tana	Europe	42000	0.113	0.040	1	52.69	0.31	8.20	0.44	4.88
Tejo	Europe	76200	0.207	0.148	1	91.21	0.39	6.43	3.71	9.00
Tocantins	South America	757000	0.491	0.003	1	4.50	0.33	1.93	0.36	1.35
Tornionjoki	Europe	39500	0.300	0.004	1	0.99	0.15	0.00	0.00	2.71
Tugela	Africa	30112	0.037	0.051	3	11.40	0.10	0.04	0.00	0.85
Uruguay	South America	240000	0.604	0.037	1	20.24	0.60	7.47	1.13	2.81
Ususmacinta	North America	47700	1.164	0.085	1	24.66	0.34	2.00	0.57	27.67
Volga	Europe	1350000	0.190	0.011	8	40.36	0.41	2.71	0.01	2.39
Weser	Europe	45800	0.247	0.370	1	190.07	0.40	19.98	3.53	75.74
Wisla	Europe	198000	0.172	0.210	1	131.88	0.26	7.26	3.04	36.98
Yana	Europe	224000	0.137	0.009	2	0.00	0.37	0.00	0.00	0.71
Yenisey	Asia	2440000	0.237	0.010	2	36.33	0.36	1.50	1.00	1.14
Yesil	Asia	35960	0.158	0.080	1	58.98	0.41	2.96	2.00	8.44
Yukon	North America	849000	0.237	0.010	1	0.09	0.33	0.00	0.00	1.91
Zaire	Africa	3698000	0.324	0.024	1	13.08	0.07	0.29	0.00	4.38
Zambezi	Africa	1330000	0.080	0.010	1	17.79	0.12	0.65	0.05	0.37
Zhujiang	Asia	437000	0.831	0.003	9	185.76	0.06	10.81	7.66	25.88

<sup>a</sup>Sources for DIP and runoff data: 1, *Meybeck and Ragu* [1996]; 2, *Holmes et al.* [2000]; 3, *Smith et al.* [2003]; 4, *United Nations Environment Programme–Mediterranean Action Plan* [2003]; 5, *Alexander et al.* [1996]; 6, *Marengo and Victoria* [1998]; 7, *Yan and Zhang* [2003]; 8, *Caraco* [1995]; 9, *Zhang et al.* [1999]. For sources of P inputs, see Table 2.

$L_{\max}$	Maximum fraction of applied manure and fertilizer P lost to coastal zone as DIP; for NEWS-DIP set equal to 0.07.	$P_{em}$	Gross human P emission, kg P person <sup>-1</sup> yr <sup>-1</sup> .
$P_{fert}$	P applied to watersheds as inorganic fertilizer, kg P km <sup>-2</sup> yr <sup>-1</sup> .	$GDP$	Gross Domestic Product, 1995 dollars yr <sup>-1</sup> .
$P_{am}$	P applied to watersheds as manure, kg P km <sup>-2</sup> yr <sup>-1</sup> .	$U$	Fraction of the population that is urban (0–1).
%Dev	Percent deviation from the 1:1 line (0–100).	$S_u$	Fraction of urban population with access to “improved sanitation” (0–1).
$Bas$	Number of distinct watersheds in analysis.	$F_{mech}$	Fraction of each country’s sewage that has mechanical treatment (0–1).
$Rt$	Change in water residence time due to dam construction, days.	$F_{biol}$	Fraction of each country’s sewage that has biological treatment (0–1).
$T$	Fraction of P from human sewage removed via wastewater treatment (0–1).	$F_{adv}$	Fraction of each country’s sewage that has advanced treatment (0–1).
$I$	Fraction of a watershed’s population connected to sewage systems (0–1).		

[52] **Acknowledgments.** We are grateful to UNESCO-IOC, the U.S. National Science Foundation, NOAA, and New Jersey Sea Grant

(ES-2002-3) for supporting this work and to Egon Dumont, Courtney Walker, and the rest of the Global NEWS working group for useful discussion and feedback. Also, the comments of two anonymous reviewers significantly enhanced the quality of this manuscript. Any opinions, findings, and conclusions or recommendations expressed in this material are those of the authors and do not necessarily reflect the views of NOAA, Sea Grant, the National Science Foundation, or other funding agencies.

## References

- Alexander, R. B., J. R. Slack, A. S. Ludtke, K. K. Fitzgerald, and T. L. Schertz (1996), Data from selected U.S. Geological Survey national stream water quality monitoring networks (WQN), *Digital Data Ser. DDS-37*, U. S. Geol. Surv., Washington, D. C.
- Alexander, R. B., P. J. Johnes, E. W. Boyer, and R. A. Smith (2002), A comparison of models for estimating the riverine export of nitrogen from large watersheds, *Biogeochemistry*, 57/58, 295–339.
- Arheimer, B., and R. Liden (2000), Nitrogen and phosphorus concentrations from agricultural catchments—Influence of spatial and temporal variables, *J. Hydrol.*, 227, 140–159.
- Baker, D. B., and R. P. Richards (2002), Phosphorus budgets and riverine phosphorus export in northwestern Ohio watersheds, *J. Environ. Qual.*, 31(1), 96–108.
- Bennett, E. M., T. Reed-Andersen, J. N. Houser, J. R. Gabriel, and S. R. Carpenter (1999), A phosphorus budget for the Lake Mendota watershed, *Ecosystems*, 2(1), 69–75.
- Bennett, E. M., S. R. Carpenter, and N. F. Caraco (2001), Human impact on erodable phosphorus and eutrophication: A global perspective, *Bioscience*, 51(3), 227–234.
- Bicknell, B. R., J. C. Imhoff, J. L. Kittle Jr., A. S. Donigan Jr., and R. C. Johanson (1997), Hydrological simulation program—Fortran, user's manual for version 11, *EPA/600/R-97/080*, 755 pp., Natl. Exposure Res. Lab., U.S. Environ. Prot. Agency, Athens, Ga.
- Billen, G., J. Garnier, A. Ficht, and C. Cun (2001), Modeling the response of water quality in the Seine River Estuary to human activity in its watershed over the last 50 years, *Estuaries*, 24(6B), 977–993.
- Black and Veach Consulting Engineers (1971), Process design manual for phosphorus removal, pp. 1-1–11-8, Black and Veach Consulting Engineers, Kansas City, Mo.
- Bouwman, A. F., G. Van Dreht, and K. W. van der Hoek (2005a), Nitrogen surface balances in intensive agricultural production systems in different world regions for the period 1970–2030, *Pedosphere*, 15(2), 137–155.
- Bouwman, A. F., G. Van Dreht, J. M. Knoop, A. H. W. Beusen, and C. R. Meinardi (2005b), Exploring changes in river nitrogen export to the world's oceans, *Global Biogeochem. Cycles*, 19, GB1002, doi:10.1029/2004GB002314.
- Boynton, W. R., J. H. Garber, R. Summers, and W. M. Kemp (1995), Inputs, transformations, and transport of nitrogen and phosphorus in Chesapeake Bay and selected tributaries, *Estuaries*, 18(1B), 285–314.
- Bradford, M. E., and H. R. Peters (1987), The relationship between chemically analyzed phosphorus fractions and bioavailable phosphorus, *Limnol. Oceanogr.*, 32, 1124–1137.
- Burwell, R. E., G. E. Schuman, H. G. Heinemann, and R. G. Spomer (1997), Nitrogen and phosphorus movement from agricultural watersheds, *J. Soil Water Conserv.*, 32, 226–230.
- Caraco, N. F. (1995), Influence of human populations on P transfers to aquatic systems: A regional scale study using large rivers, in *Phosphorus in the Global Environment: Transfers, Cycles and Management (SCOPE 54)*, edited by H. Tiessen, pp. 236–244, John Wiley, Hoboken, N. J.
- Caraco, N. F., and J. J. Cole (1999), Human impact on nitrate export: An analysis using major world rivers, *Ambio*, 28, 167–170.
- Chapra, S., and G. Pelletier (2003), A modeling framework for simulating river and stream water quality: Documentation and users manual, report, pp. 1–127, Civ. and Environ. Eng. Dep., Tufts Univ., Medford, Mass.
- Cooper, D. M., W. A. House, L. May, and B. Gannon (2002), The phosphorus budget of the Thames catchment, Oxfordshire, UK: 1. Mass balance, *Sci. Total Environ.*, 282–283, 233–251.
- Daly, K., P. Mills, B. Coulter, and M. McGarrigle (2002), Modeling phosphorus concentrations in Irish rivers using land use, soil type, and soil phosphorus data, *J. Environ. Qual.*, 31, 590–599.
- Dumont, E., J. A. Harrison, C. Kroeze, E. J. Bakker, and S. P. Seitzinger (2005), Global distribution and sources of DIN export to the coastal zone: Results from a spatially explicit global model, *Global Biogeochem. Cycles*, in press.
- Ebeling, A. M., L. G. Bundy, M. J. Powell, and T. W. Andraski (2002), Dairy diet phosphorus effects on phosphorus losses in runoff from land-applied manure, *Soil Sci. Soc. Am. J.*, 66, 284–291.
- Eklholm, P. (1994), Bioavailability of phosphorus in agriculturally loaded rivers in southern Finland, *Hydrobiologia*, 287, 179–194.
- Fisher, T. R., A. B. Gustafson, K. Sellner, R. Lacouture, L. W. Haas, R. L. Wetzel, R. Magnien, D. Everitt, B. Michaels, and R. Karrh (1999), Spatial and temporal variation of resource limitation in Chesapeake Bay, *Mar. Biol.*, 133(4), 763–778.
- Fixen, P. E., and F. B. West (2002), Nitrogen fertilizers: Meeting contemporary challenges, *Ambio*, 31, 169–176.
- Fox, L. E. (1989), A model for inorganic control of phosphate concentrations in river waters, *Geochim. Cosmochim. Acta*, 53, 417–428.
- Froelich, P. N. (1988), Kinetic control of dissolved phosphate in natural rivers and estuaries: A primer on the phosphate buffer mechanism, *Limnol. Oceanogr.*, 33, 649–668.
- Green, P. A., C. J. Vörösmarty, M. Meybeck, J. N. Galloway, B. J. Peterson, and E. W. Boyer (2004), Pre-industrial and contemporary fluxes of nitrogen through rivers: A global assessment based on typology, *Biogeochemistry*, 68, 71–105.
- Harrison, P. J., M. H. Hu, Y. P. Yang, and X. Lu (1990), Phosphate limitation in estuarine and coastal waters of China, *J. Exp. Mar. Biol. Ecol.*, 140, 79–87.
- HELCOM (2003), Executive summary of the Fourth Baltic Sea Pollution Load Compilation (PLC-4), Helsinki Comm. Baltic Mar. Environ. Prot. Comm., Helsinki.
- Holmes, R. M., B. J. Peterson, V. V. Gordeev, A. V. Zhulidov, M. Meybeck, R. B. Lammers, and C. J. Vörösmarty (2000), Flux of nutrients from Russian rivers to the Arctic Ocean: Can we establish a baseline against which to judge future changes?, *Water Resour. Res.*, 36(8), 2309–2320.
- Howarth, R., H. Jensen, R. Marino, and H. Postma (1995), Transport to and processing of phosphorus in near-shore and oceanic waters, in *Phosphorus in the Global Environment: Transfers, Cycles and Management (SCOPE 54)*, edited by H. Tiessen, pp. 323–345, John Wiley, Hoboken, N. J.
- Howarth, R. W., et al. (1996), Regional nitrogen budgets and riverine N&P fluxes for the drainages to the North Atlantic Ocean: Natural and human influences, *Biogeochemistry*, 35, 75–139.
- Jensen, H. S., K. J. McGlathery, R. Marino, and R. W. Howarth (1998), Forms and availability of sediment phosphorus in carbonate sand of Bermuda seagrass beds, *Limnol. Oceanogr.*, 43, 799–810.
- Jordan, T. E., D. E. Weller, and D. L. Correll (2003), Sources of nutrient inputs to the Patuxent River Estuary, *Estuaries*, 26(2A), 226–243.
- Justic, D., N. N. Rabalais, and R. E. Turner (1995), Stoichiometric nutrient balance and origin of coastal eutrophication, *Mar. Pollut. Bull.*, 30, 41–46.
- Klein Goldewijk, K. (2001), Estimating historical land use changes over the past 3000 years: The HYDE database, *Global Biogeochem. Cycles*, 15(2), 417–434.
- Kroeze, C., and S. P. Seitzinger (1998), Nitrogen inputs to rivers, estuaries and continental shelves and related nitrous oxide emissions in 1990 and 2050: A global model, *Nutr. Cycling Agroecosyst.*, 52(2–3), 195–212.
- Mackenzie, F. T., L. M. Ver, and A. Lerman (1998), Coupled biogeochemical cycles of carbon, nitrogen, phosphorus and sulfur in the land-ocean-atmosphere system, in *Asian Change in the Context of Global Climate Change*, edited by J. N. Galloway and J. M. Melillo, Cambridge Univ. Press, New York.
- Marengo, J. A., and R. L. Victoria (1998), *Carbon in the Amazon River Experiment- (CAMREX) data on Pre-LBA Data Sets Initiative* [CD-ROM], Cent. de Previsao de Tempo e Estudos Clim., Inst. Nacl. de Pesqui. Espaciais (CPTEC/INPE), Sao Paulo, Brazil. (Available at <http://lba.cptec.inpe.br/>)
- McCull, R. H. S., E. White, and A. R. Gibson (1977), Phosphorus and nitrate runoff in hill pasture and forest catchments, *Mar. Freshwater Res.*, 11, 729–744.
- McDowell, L. L., and K. C. McGregor (1984), Plant nutrient losses in runoff from conservation tillage corn, *Soil Tillage Res.*, 4, 79–91.
- McIntyre, N. R., T. Wagener, H. S. Wheaton, and S. C. Chapra (2003), Risk-based modelling of surface water quality: A case study of the Charles River, Massachusetts, *J. Hydrol.*, 274, 225–247.
- Melack, J. M. (1995), Transport and transformations of P, fluvial and lacustrine ecosystems, in *Phosphorus in the Global Environment: Transfers, Cycles and Management (SCOPE 54)*, edited by H. Tiessen, pp. 245–254, John Wiley, Hoboken, N. J.
- Meybeck, M. (1982), Carbon, nitrogen, and phosphorus transport by world rivers, *Am. J. Sci.*, 282, 401–450.
- Meybeck, M., and A. Ragu (1996), River discharges to the oceans: An assessment of suspended solids, major ions, and nutrients, in *Environment Information and Assessment*, pp. 1–245, U.N. Environ. Programme, Paris.

- Moore, R. B., C. M. Johnston, K. W. Robinson, and J. R. Deacon (2004), Estimation of total nitrogen and phosphorus in New England Streams using spatially referenced regression models, *Sci. Invest. Rep. 2004-5012*, 41 pp., U.S. Geol. Surv., Pembroke, N. H.
- Murrell, M. C., R. S. Stanley, E. M. Loes, G. T. DiDonato, L. M. Smith, and D. A. Flemer (2002), Evidence that phosphorus limits phytoplankton growth in a Gulf of Mexico estuary: Pensacola Bay, Florida, USA, *Bull. Mar. Sci.*, 70, 155–167.
- Nash, J. E., and J. V. Sutcliffe (1970), River flow forecasting through conceptual models: 1. A discussion of principles, *J. Hydrol.*, 10, 282–290.
- Neitsch, S. L., J. G. Arnold, J. R. Kiniry, R. Srinivasan, and J. R. Williams (2002), Soil and water assessment tool user's manual, version 2000, *TWRI Rep. TR-192*, 472 pp., Texas Water Resour. Inst., College Station, Tex.
- Nicholaichuk, W., and D. W. L. Read (1978), Nutrient runoff from fertilized and unfertilized fields in western Canada, *J. Environ. Qual.*, 7, 542–544.
- Pierrou, U. (1975), The global phosphorus cycle, in *Nitrogen, Phosphorus, and Sulfur—Global Cycles*, edited by B. H. Svensson and R. Soderlund, pp. 75–88, Sci. Comm. on Problems of the Environ., Stockholm.
- Richey, J. E. (1983), The phosphorus cycle, in *The Major Biogeochemical Cycles and Their Interactions*, edited by E. T. Degens, S. Kempe, and J. E. Richey, pp. 51–56, John Wiley, Hoboken, N. J.
- Seitzinger, S. P., and C. Kroeze (1998), Global distribution of nitrous oxide production and N inputs in freshwater and coastal marine ecosystems, *Global Biogeochem. Cycles*, 12(1), 93–113.
- Seitzinger, S. P., C. Kroeze, A. F. Bouman, N. Caraco, F. Dentener, and R. V. Styles (2002), Global patterns of dissolved inorganic and particulate nitrogen inputs to coastal systems: Recent conditions and future projections, *Estuaries*, 25(4B), 640–655.
- Sharpley, A. N., and J. K. Syers (1979), Phosphorus inputs into a stream draining an agricultural watershed: II. Amounts and relative significance of runoff types, *Water Air Soil Pollut.*, 11, 417–428.
- Sharpley, A. N., M. J. Hedley, E. Sibbesen, A. Hillbricht-Ilkowska, W. A. House, and L. Ryszkowski (1995), Phosphorus transfers from terrestrial to aquatic ecosystems, in *Phosphorus in the Global Environment: Transfers, Cycles and Management (SCOPE 54)*, edited by H. Tiessen, pp. 171–199, John Wiley, Hoboken, N. J.
- Slam, M. A. (1980), Mechanistic and practical aspects of phosphorus removal from wastewater using iron (III) salts, Master's thesis, Rutgers—The State University of New Jersey, New Brunswick.
- Smith, S. V., et al. (2003), Humans, hydrology, and the distribution of inorganic nutrient loading to the ocean, *Bioscience*, 53(3), 235–245.
- Turner, R. E., N. N. Rabalais, D. Justic, and Q. Dortch (2003), Global patterns of dissolved N, P and Si in large rivers, *Biogeochemistry*, 64, 297–317.
- United Nations Environment Programme—Mediterranean Action Plan (2003), Riverine transport of water, sediments and pollutants to the Mediterranean Sea, *MAP Tech. Rep. 141*, 111 pp., Athens.
- Van Drecht, G., A. F. Bouwman, J. M. Knoop, A. H. W. Beusen, and C. R. Meinardi (2003), Global modeling of the fate of nitrogen from point and nonpoint sources in soils, groundwater, and surface water, *Global Biogeochem. Cycles*, 17(4), 1115, doi:10.1029/2003GB002060.
- Ver, L. M., F. T. MacKenzie, and A. Lerman (1999), Biogeochemical responses of the carbon cycle to natural and human perturbations: Past, present, and future, *Am. J. Sci.*, 299, 762–801.
- Viney, N. R., M. Sivapalan, and D. Deeley (2000), A conceptual model of nutrient mobilisation and transport applicable at large catchment scales, *J. Hydrol.*, 240, 23–44.
- Vörösmarty, C. J., K. Sharma, B. Fekete, A. H. Copeland, J. Holden, J. Marble, and J. A. Lough (1997), The storage and aging of continental runoff in large reservoir systems of the world, *Ambio*, 26, 210–219.
- Vörösmarty, C. J., B. M. Fekete, M. Meybeck, and R. Lammers (2000a), A simulated topological network representing the global system of rivers at 30-minute spatial resolution (STN-30), *Global Biogeochem. Cycles*, 14(2), 599–621.
- Vörösmarty, C. J., B. M. Fekete, M. Meybeck, and R. B. Lammers (2000b), Geomorphometric attributes of the global system of rivers at 30-minute spatial resolution, *J. Hydrol.*, 237, 17–39.
- Vörösmarty, C. J., M. Meybeck, B. M. Fekete, K. Sharma, P. Green, and J. P. M. Syvitski (2003), Anthropogenic sediment retention: Major global impact from registered river impoundments, *Global Planet. Change*, 39, 169–190.
- Weller, D. E., T. E. Jordan, D. L. Correll, and Z.-J. Liu (2003), Effects of land-use change on nutrient discharges from the Patuxent River watershed, *Estuaries*, 26(2A), 244–266.
- Wilhelmus, B., M. Bernhardt, and P. Neuman (1978), Vergleichende untersuchungen über die phosphoreliminierung von vorsperren - Verminderung der algenentwicklung in speicherbecken und talsperren, deutscher verein gas wasser-fach, *Schriften: Wasser*, 16, 140–176.
- Wollast, R. (1983), Interactions in estuaries and coastal waters, in *The Major Biogeochemical Cycles and Their Interactions*, edited by B. Bolin and R. B. Cook, pp. 385–410, John Wiley, Hoboken, N. J.
- Wool, T. A., R. B. Ambrose, J. L. Martin, and E. A. Comer (2004), Water quality analysis simulation program (WASP), version 6.0, 267 pp., U.S. Environ. Prot. Agency, Washington, D. C.
- World Bank (2000), *The 2000 World Bank Development Indicators [CD-ROM]*, Washington, D. C.
- World Health Organization/UNICEF (2001), Joint monitoring programme for water supply and sanitation: Coverage estimates 1980–2000, report, Geneva.
- Yan, W. J., and S. Zhang (2003), The composition and bioavailability of phosphorus transport through the Changjiang (Yangtze) River during the 1998 flood, *Biogeochemistry*, 65, 179–194.
- Zhang, J., Z. G. Yu, J. T. Wang, J. L. Ren, H. T. Chen, H. Xiong, L. X. Dong, and W. Y. Xu (1999), The subtropical Zhujiang (Pearl River) Estuary: Nutrient, trace species and their relationship to photosynthesis, *Estuarine Coastal Shelf Sci.*, 49(3), 385–400.

A. H. W. Beusen and A. F. Bouwman, Netherlands Environmental Assessment Agency (MNP), P.O. Box 303, NL-3720 AH Bilthoven, Netherlands. (arthur.beusen@mnp.nl; lex.bouwman@mnp.nl)

N. Caraco, Institute of Ecosystem Studies, Box AB, Route 44a, Millbrook, NY 12545-0128, USA. (caracon@ecostudies.org)

J. A. Harrison and S. P. Seitzinger, Institute of Marine and Coastal Sciences, Rutgers—The State University, 71 Dudley Road, New Brunswick, NJ 08901-8521, USA. (harrison@imcs.rutgers.edu; sybil@imcs.rutgers.edu)

C. J. Vörösmarty, Water Systems Analysis Group, Complex Systems Research Center, Institute for the Study of Earth, Oceans, and Space, University of New Hampshire, Durham, NH 03824, USA. (charles.vorosmarty@unh.edu)

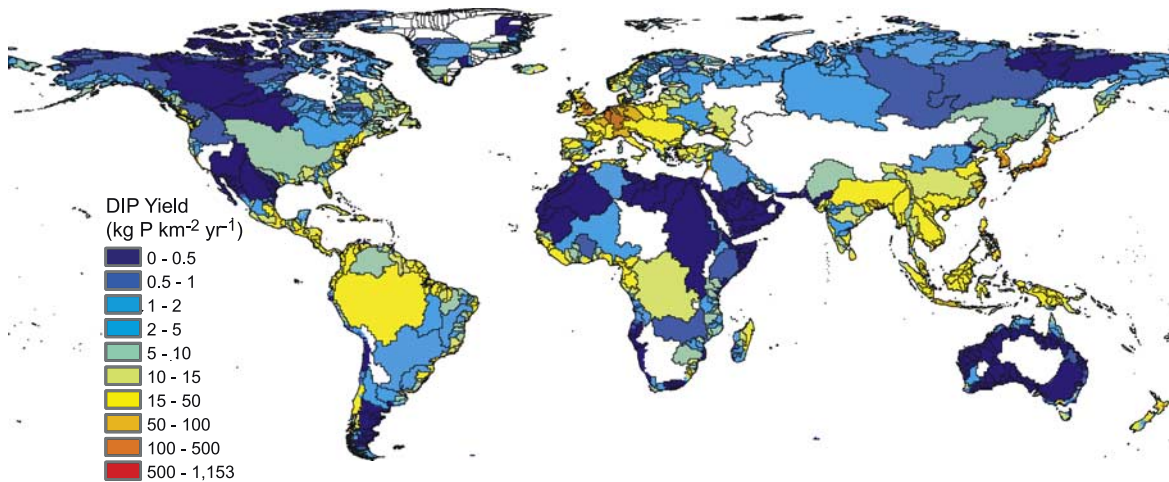


**Figure 3.** NEWS-DIP predicted DIP yield by watershed (kg P km<sup>-2</sup> yr<sup>-1</sup>) for exoreic basins. White basins are either endoreic or had no predicted DIP export. For the sake of clarity, only delineations for basins containing more than 10 half-degree grid cells are shown.

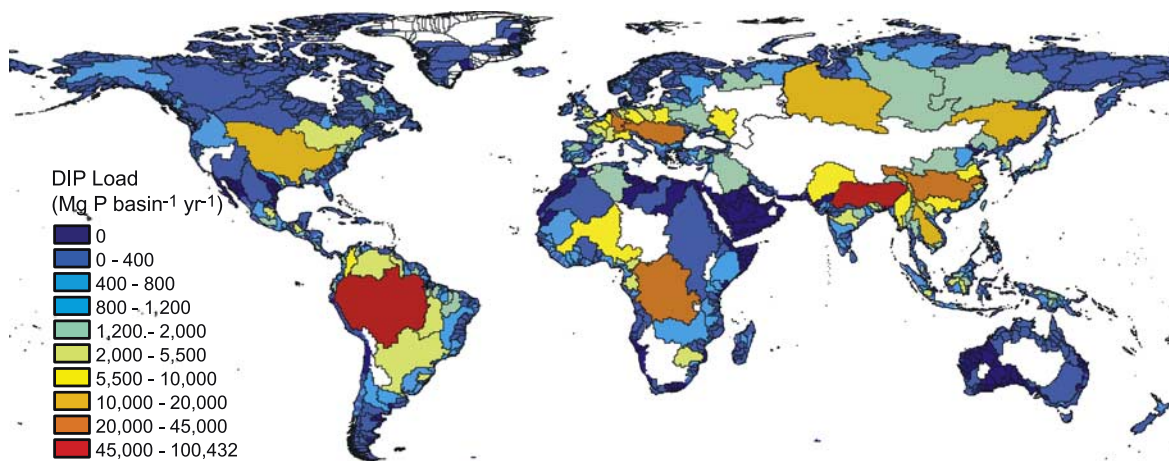


**Figure 4.** NEWS-DIP predicted DIP load by watershed (Mg P basin<sup>-1</sup> yr<sup>-1</sup>) for exoreic basins. For the sake of clarity, only delineations for basins containing more than 10 half-degree grid cells are shown.

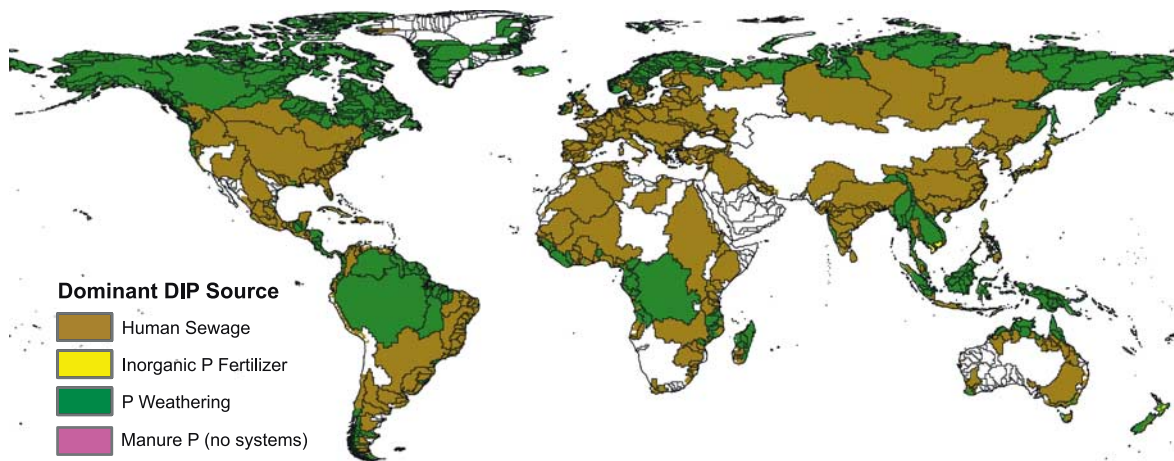


**Figure 5.** Dominant source of DIP by watershed for exoreic basins. “Dominant source” is defined as the modeled source that NEWS-DIP predicts contributes the largest fraction of DIP to the coast. For the sake of clarity, only delineations for basins containing more than 10 half-degree grid cells are shown.